Conformational Characteristics, Configurational Properties, and Thermodynamic Characteristics of Poly(ethylene terephthalate) and Poly(ethylene-2,6-naphthalate)

Yuji Sasanuma*

Department of Applied Chemistry and Biotechnology, Faculty of Engineering, Chiba University, 1-33 Yayoi-cho, Inage-ku, Chiba 263-8522, Japan

Received December 17, 2008; Revised Manuscript Received January 25, 2009

ABSTRACT: Conformational analysis of poly(ethylene terephthalate) (PET) and poly(ethylene-2,6-naphthalate) (PEN) has been carried out by the refined rotational isomeric state (RIS) scheme coupled with ab initio molecular orbital (MO) calculations for a model compound, ethylene glycol dibenzoate (EGDB). ^{1}H and ^{13}C NMR experiments for unlabeled and ^{13}C-labeled EGDBs yielded bond conformations of the central O−CH_2−CH_2−O bond sequence. The MO calculations satisfactorily reproduced not only the experimental bond conformations but also the dipole moment and molar Kerr constant observed from EGDB. The aromatic ring and ester group of EGDB render its intramolecular interactions more complicated than those of poly(ethylene oxide) with the same O−CH_2−CH_2−O bonds; C═O···H−C and C−O···H−C close contacts and dipole−dipole interactions are simultaneously formed in EGDB. The characteristic ratio of PET, derived from the refined RIS calculations using the MO energies for EGDB, exactly agree with those determined from small angle neutron scattering experiments for the melt. Thermodynamic quantities on PET and PEN, evaluated from the RIS calculations, have well characterized melting and crystallization behaviors of these polyesters.

Introduction

Poly(ethylene terephthalate) (PET, Figure 1a) is the most common polyester, usually molded into fibers, films, and bottles, and widely used in our daily lives.[1] Poly(ethylene-2,6-naphthalate) (PEN, Figure 1b) was developed in the expectation that strong intermolecular cohesions around its naphthyl rings would lead to physical properties superior to PET and has been used mainly as rigid thermoplastic films.[2]

In 1967, Williams and Flory[3] reported conformational analysis of PET. They defined conformational energies (E_ρ, E_σ, and E_ω) for the O−CH_2−CH_2−O bond sequence (hereafter referred to as 'spacer' as often used for main-chain liquid crystals) in a similar manner for poly(ethylene oxide) (PEO).[4−7] The E_ρ and E_σ values correspond to gauche−trans energy differences of the O−CH_2 and CH_2−CH_2 bonds, respectively, and the E_ω parameter represents the second-order pentane-effect-like interaction formed in $g^{\pm}g^{\mp}$ conformations for the O−CH_2/CH_2−CH_2 bond pairs.[8] The cis−trans energy difference (E_γ) of the terephthaloyl part was assumed to be negligible. In their analysis, the energy parameters were adjusted so as to reproduce an experimental characteristic ratio ($\langle r^2\rangle_0/nl^2$) of 4.6.[9,10] The optimized energy parameters of $E_\rho = 0.4_2$, $E_\sigma = -0.2_4$, $E_\omega = 1.4$, and $E_\gamma = 0.0$ kcal mol^{-1} yielded a somewhat smaller $\langle r^2\rangle_0/nl^2$ value of 4.1.[3]

Difficulties in conformational analysis of PET are partly due to its low solubility. Table 1 shows typical good solvents that have been used in viscometric measurements for PET: trifluoroacetic acid (TFA), phenol/trichlorophenol, phenol/tetrachloroethane, and *o*-chlorophenol, and dichloroacetic acid. Unperturbed chain dimensions of PET have been indirectly estimated by the Kurata−Stockmayer[11] and Stockmayer−Fixman[12] plots for viscometric data obtained from such solutions; the representative experimental data[10,13−16] are presented in Table 1. The $\langle r^2\rangle_0/nl^2$ values thus derived are considerably scattered. In addition to the characteristic ratio, the dipole moment ratio, measured with nonpolar solvents, has often been adopted as a configuration-dependent parameter in conformational analyses of polymers.[17] However, the experimental dipole moment is unavailable from PET because it is insoluble in nonpolar solvents. The molar Kerr constant, obtained from electrical birefringence and depolarized Rayleigh scattering measurements, has been expected to be utilized as a configuration-dependent

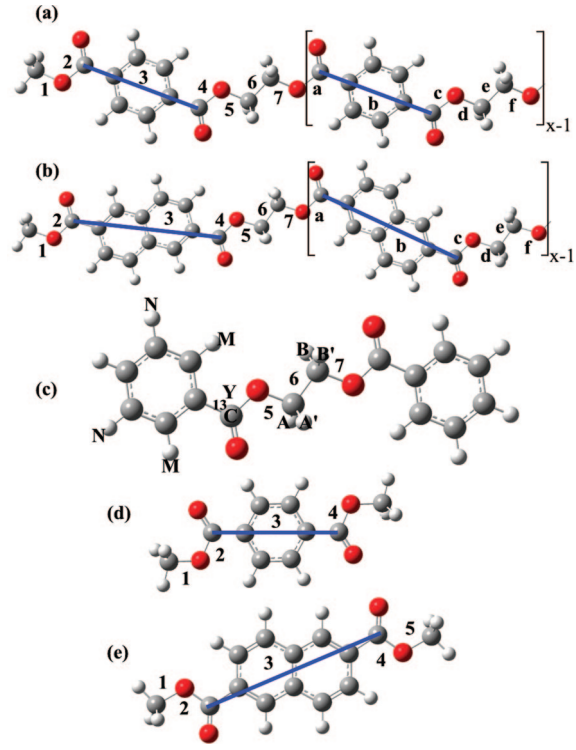

Figure 1. All-trans states of (a) poly(ethylene terephthalate) (PET), (b) poly(ethylene-2,6-naphthalate) (PEN), (c) ethylene glycol dibenzoate (EGDB), (d) dimethyl terephthalate (DMT), and (e) dimethyl 2,6-naphthalate (DMN). The thick line segments express virtual bonds of the aromatic rings. The bonds are labeled as indicated. The hydrogen and carbon atoms of EGDB are partly designated to represent spin systems of ^{1}H and ^{13}C NMR spectra shown in Figure 3 (see text).

* Corresponding author. E-mail: sasanuma@facutly.chiba-u.jp. Fax: +81 43 290 3394.

10.1021/ma802804n CCC: $40.75
Published on Web 03/18/2009

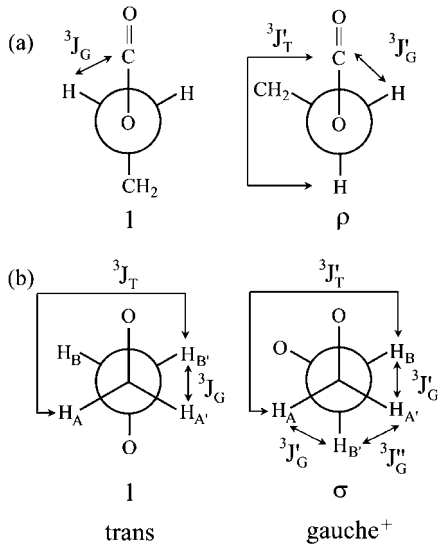

Figure 2. Rotational isomeric states around (a) O−CH$_2$ and (b) CH$_2$−CH$_2$ bonds of the spacers of EGDB, PET, and PEN with definitions of vicinal trans (^3J_T) and gauche (^3J_G) coupling constants. The Greek letters, ρ and σ, represent first-order interactions.

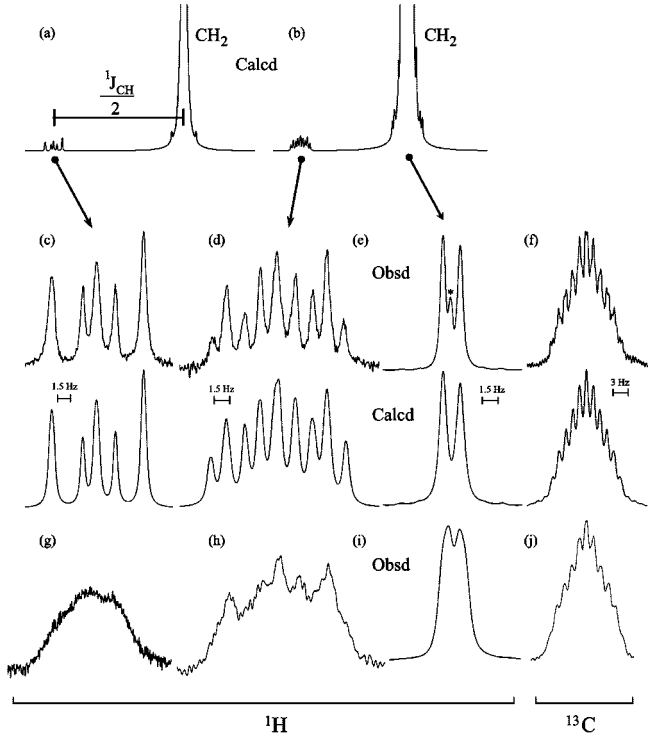

Figure 3. ^{1}H and ^{13}C NMR spectra of EGDB and EGDB-$^{13}C_1$ in benzene-d_6 at 35 °C (a−f) and in TFA-d at 35 °C (g−j). For the details, see text. The asterisk in part e indicates a peak from an impurity, unlabeled EGDB.

parameter for conformational analysis of polymers.[17−23] In the early 1980s, Flory and co-workers[24,25] revisited conformations of aromatic esters to determine dipole moment vectors and excess polarizabilities of benzoates and terephthalates for conformational analysis of aromatic polyesters by means of the molar Kerr constant. Unfortunately, his challenge was terminated by his death before reaching aromatic polyesters.

It is a generally accepted concept that molten polymers lie in the Θ state.[26] Small-angle neutron scattering (SANS) experiments have been conducted for polymer melts to determine unperturbed chain dimensions.[27,28] Table 1 also shows SANS observations for molten PET.[29] The SANS experiments, based on two preceding studies,[30,31] adopted elaborate sample preparation: melt-pressing to depress scattering from voids, melting at 250 °C to avoid both transesterification and crystallization, and quenching in ice−water. The sample was expected to keep the unperturbed amorphous state at 250 °C. The $\langle r^2\rangle_0/nl^2$ values determined from the SANS measurements are smaller than those obtained from the solutions.

Table 1. Experimental Characteristic Ratios of PET[a]

method	$\langle r^2\rangle_0/nl^2$ [b]	solvent, state	temp, °C	ref
viscosity	5.2	PH/TrCPH	30	10
	4.0, 4.1	TFA	30	13
	4.3, 4.5	PH/TeCE	30	13
	4.2	PH/TeCE	25	14
	2.3, 3.5, 3.7	*o*-chlorophenol	25	15
	4.0	DCA/CH	25	16
SANS	2.7, 3.1	amorphous (melt)	250	29

[a] Abbreviations: TFA, trifluoroacetic acid; PH, phenol; TrCPH, trichlorophenol; TeCE, tetrachloroethane; DCA, dichloroacetic acid; CH, cyclohexane; SANS, small-angle neutron scattering. [b] The $\langle r^2\rangle_0/nl^2$ values calculated with bond lengths determined here (Table 8), multiplied by nl^2/M (43.5/192 Å^2 g^{-1} mol) of the repeating unit, can be converted to $\langle r^2\rangle_0/M$.

After Flory's work, a number of studies have dealt with conformations of PET and related compounds; some studies employed the Williams−Flory model as it is, some modified it, some proposed different simulation models, and some reported new experimental data. For example, Riande et al.[32] reported a comparative study of the polarity of PET and poly(propyleneglycol terephthalate). Mattice et al.[33] related intramolecular excimer formation of aromatic polyesters including PET to their conformational dynamics. Saiz et al.[34] measured dipole moments and molar Kerr constants of model compounds of aromatic polyesters, $C_6H_5COO(CH_2)_mOOCC_6H_5$ ($m = 2-6$). Vacatello et al.[35] carried out Monte Carlo simulations of PET. Stepto et al.[36] performed the rotational isomeric state (RIS) and Metropolis Monte Carlo simulations of PET. Tonelli[37] conducted the RIS calculations for PET, poly(ethylene isophthalate), poly(ethylene phthalate), and PEN. Kamio et al.[38] proposed a coarse-grained model for molten PET. However, the results presented so far are not necessarily consistent with each other.

This study aims to reveal conformational characteristics and configurational properties of PET and PEN in a different way from the preceding work and resolve the confusion. As a model compound for repeating units of PET and PEN, ethylene glycol dibenzoate (EGDB) has been adopted here (see Figure 1c). ^{1}H and ^{13}C NMR spectra of EGDB containing a ^{13}C-labeled ester group (EGDB-$^{13}C_1$) were measured and analyzed to yield bond conformations of O−CH$_2$ and CH$_2$−CH$_2$ bonds in the spacer. Density functional and ab initio molecular orbital (MO) calculations were carried out for all possible conformers of EGDB in vacuo and in benzene to evaluate free energies, dipole moments, and polarizabilities. Energy differences (E_γ's) between trans and cis forms around aromatic rings of PET and PEN were derived from those of dimethyl terephthalate (DMT, Figure 1d) and dimethyl 2,6-naphthalate (DMN, Figure 1e), respectively. The bond conformations, dipole moment, and molar Kerr constant of EGDB were calculated from the MO data and compared with experiments. On the grounds of good agreement between theory and experiment, the conformer free energies were broken down into conformational energies, and intramolecular interactions found for EGDB were investigated. Configurational properties and thermodynamic quantities of PET and PEN were evaluated from the refined RIS calculations and compared with experimental observations. Conformational characteristics, solution and melt properties, and melting and crystallization of these polyesters are discussed in this paper.

Computations and Experiments

MO Calculations. Density functional and ab initio MO calculations were carried out with the Gaussian03 program[39] installed on an HPC Silent-SCC T2 or an HPC SCC System-L computer. For each conformer of EGDB, geometrical parameters were fully optimized at the B3LYP/6-311+G(2d, p) level, and the thermal-correction term to the Gibbs free energy (at 25 and 250 °C), dipole moment, and polarizability were calculated concomitantly. All self-consistent field (SCF) calculations were conducted under the tight convergence. With the optimized geometry, the SCF energy (MP2 (SCF)) was computed at the MP2/6-311+G(2d, p) level. The Gibbs free energy was evaluated from the MP2 (SCF) and thermal-correction energies, being given here as the difference from that of the all-trans conformer and denoted as ΔG_k (k: conformer). Free energy differences between cis and trans states of DMT and DMN were evaluated in the same manner. The ΔG_k values for benzene environments at 25 and 250 °C were also calculated at the MP2/6-311+G(2d, p) level with the integral equation formalism of the polarizable continuum model (IEF-PCM).[40,41] The MO data on the benzene solution at 250 °C (over the boiling point) may represent the solute molecule surrounded by media of the permittivity of benzene. The molecular geometry and thermal correction term for the gas phase were also used for the benzene environments because geometrical optimization using the IEF-PCM theory for EGDB occasionally failed to converge.

Vicinal ^{1}H−^{1}H and ^{13}C−^{1}H coupling constants of EGDB, used in ^{1}H and ^{13}C NMR analyses, were calculated at the B3LYP/6-311++G(3df, 3pd)//B3LYP/6-311+G(2d, p) level. Bond lengths, bond angles, and dihedral angles used in the refined RIS computations[42,43] for PET and PEN were determined by geometrical optimization at the B3LYP/6-31G(d) level for conformers of ethyleneglycol bis(dimethyl terephthalate) and ethyleneglycol bis-(dimethyl 2,6-naphthalate), respectively (see Tables S1 and S2, Supporting Information).

Sample Preparation. Unlabeled ethylene glycol dibenzoate was prepared as described in the literature.[44] Ethylene glycol dibenzoate-$^{13}C_1$ was synthesized as follows. Benzoyl-*carbonyl*-^{13}C chloride (Isotec, 99 atom % ^{13}C, 1 g, 7 mmol) was added dropwise through a 1 mL syringe to anhydrous pyridine (0.8 g, 10 mmol) and ethylene glycol monobenzoate (1.7 g, 10 mmol) prepared beforehand[44] in a flask equipped with a reflux condenser and a thermometer. After being allowed to stand at room temperature for 2 h, the reaction mixture was heated up slowly, kept at 70 °C for 2 h, and cooled down to room temperature. The mixture underwent extraction with ether and water. The ether layer was washed three times with 5% aqueous sodium bicarbonate, dried overnight over anhydrous magnesium sulfate, and filtered. The ether was removed in a rotary evaporator. The residue was recrystallized from absolute ethanol to yield EGDB-$^{13}C_1$.

NMR Measurements. H (^{13}C) NMR spectra were recorded at 500 MHz (126 MHz) on a JEOL JNM-LA500 spectrometer equipped with a variable temperature controller in the Chemical Analysis Center of Chiba University. The measurement temperatures were 15, 25, 35, 45, and 55 °C and maintained within ± 0.1 °C fluctuations. Free induction decays were accumulated 64 (256) times. The $\pi/2$ pulse width, data acquisition time, and recycle delay were 5.6 (5.0) μs, 6.6 (1.9) s, and 2.0 (2.0) s, respectively. Here, the values in the parentheses are ^{13}C NMR parameters. The gated decoupling technique was employed in the ^{13}C NMR experiments. The solvents were cyclohexane-d_{12}, benzene-d_6, methanol-d_4, dimethyl-d_6 sulfoxide, and trifluoroacetic acid-d and the solute concentration was ca. 5 vol %. The NMR spectra were simulated with the gNMR program[45] to derive chemical shifts and coupling constants.

Results and Discussion

^{1}H and ^{13}C NMR of EGDB and EGDB-$^{13}C_1$. Figure 2 illustrates that the vicinal ^{13}C−^{1}H coupling constant ($^3J_{CH}$) can be expressed as a function of trans (p_t) and gauche (p_g) fractions of the O−CH_2 bond in the spacer:

$$^3J_{CH} = {}^3J_G p_t + \frac{{}^3J'_T + {}^3J'_G}{2} p_g \quad (1)$$

Here, $^3J'_T$, ^3J_G, and $^3J'_G$, defined in Figure 2, are vicinal trans and gauche coupling constants, respectively. The definition of bond conformations leads to

$$p_t + p_g = 1 \quad (2)$$

For methylene protons of EGDB, two vicinal ^{1}H−^{1}H coupling constants determined experimentally, $^3J_{HH}$ (= $^3J_{AB}$ = $^3J_{A'B'}$) and $^3J'_{HH}$ (= $^3J_{AB'}$ = $^3J_{A'B}$), are related to trans and gauche fractions of the CH_2−CH_2 bond in the spacer:

$$^3J_{HH} = {}^3J_G p_t + \frac{{}^3J'_T + {}^3J''_G}{2} p_g \quad (3)$$

and

$$^3J'_{HH} = {}^3J_T p_t + {}^3J'_G p_g \quad (4)$$

where ^3J_T's and ^3J_G's are illustrated in Figure 2. To derived p_t and p_g values of the O−CH_2 and CH_2−CH_2 bonds from the above equations, ^{1}H and ^{13}C NMR spectra of both EGDB and EGDB-$^{13}C_1$ were measured and analyzed.

Shown in Figure 3c is one of two ^{1}H NMR satellite bands of EGDB, appearing at a remove of $^1J_{CH}/2$ from the intense methylene singlet (Figure 3a). Figure 3 also shows a ^{1}H NMR spectra of methylene groups of EGDB-$^{13}C_1$. The main signal (Figure 3e) is a doublet, and its satellite band (Figure 3d) comprises more peaks than that of EGDB, because the ^{13}C-labeled carbonyl carbon and phenyl protons as well as the four methylene protons form spin−spin couplings and yield a number of signals. Figure 3f shows an observed ^{13}C NMR spectrum of the ^{13}C-labeled carbonyl carbon; it exhibits a fine structure due to ^{13}C−^{1}H couplings with the methylene and phenyl protons. The spin systems of spectra in parts c, d (e), and f of Figure 3 may be expressed as AA′BB′(X), AA′BB′M_2(X)Y, and AA′BB′M_2N_2Y, respectively (A, A′, B, and B′, methylene protons; M and N, phenyl protons, (X), natural-abundance methylene carbon; Y, ^{13}C-labeled carbonyl carbon. For the assignment, see Figure 1c). It is reasonable to assume that the four spectra (Figures 3c−f), measured with the same solvent at the same temperature, can be reproduced by a set of ^{1}H−^{1}H and ^{13}C−^{1}H coupling constants; accordingly, the following analytic procedure was employed.

First, spectrum c was simulated with the gNMR program to yield the $^3J_{HH}$ and $^3J'_{HH}$ values. With these coupling constants, spectra d and e were analyzed to derive the $^3J_{CH}$ value. Spectrum f was confirmed to be satisfactorily reproduced from the ^3J data, and, furthermore, both chemical shifts and coupling constants were adjusted until the best agreement was attained for all the spectra. For comparison, the calculated spectra are also shown in Figure 3, and the coupling constants were optimized as follows: $^3J_{HH}$ = 6.50, $^3J'_{HH}$ = 3.10, $^3J_{CH}$ = 3.32, $^1J_{CH}$ = 145.85, $^3J_{YM}$ = 4.10, $^4J_{YN}$ = 1.10, and $^4J_{YB}$ = −0.30 Hz. The $^3J_{HH}$, $^3J'_{HH}$, and $^3J_{CH}$ values for all the solutions are listed in Table 2. Figures 3g−j show low-resolution spectra observed from the TFA solution. The broadening reflects a rapid relaxation due to the viscosity of TFA and/or some EGDB···TFA interaction. As mentioned in the Introduction, TFA is one of the few good solvents used in viscometry for PET to determine the chain dimension and molecular weight.

According to eqs 2−4, bond conformations of the CH_2−CH_2 bond in the spacer were evaluated from the $^3J_{HH}$ and $^3J'_{HH}$ values. Then, the coefficients (^3J_T's and ^3J_G's) in eqs 3 and 4 were taken from (set A) those optimized for 1,2-dimethoxyethane and

Table 2. Observed Vicinal $^1H-^1H$ and $^{13}C-^1H$ Coupling Constants of EGDB and EGDB-$^{13}C_1$[a]

solvent	dielectric constant	temp, °C	$^3J_{HH}$	$^3J'_{HH}$	$^3J_{CH}$
cyclohexane-d_{12}	2.0	15	6.42	3.37	3.37
		25	6.43	3.47	3.38
		35	6.45	3.54	3.41
		45	6.46	3.62	3.42
		55	6.48	3.65	3.43
benzene-d_6	2.3	15	6.55	3.00	3.25
		25	6.50	3.05	3.30
		35	6.50	3.10	3.32
		45	6.45	3.15	3.35
		55	6.45	3.25	3.36
methanol-d_4	32.7	15	6.55	2.75	3.40
		25	6.50	2.85	3.45
		35	6.45	2.95	3.45
		45	6.40	3.05	3.45
		55	6.40	3.10	3.47
dimethyl-d_6 sulfoxide	46.7	15	6.45	2.60	3.20
		25	6.45	2.70	3.25
		35	6.45	2.76	3.25
		45	6.45	2.80	3.30
		55	6.45	2.90	3.35
trifluoroacetic acid-d[b]	-				

[a] In Hz. [b] The trifluoroacetic acid solution also underwent NMR measurements at 15−55 °C but did not give enough resolution to yield the coupling constants (see Figure 3).

PEO,[46] (set B) those of *cis*-2,6-dimethyl-1,4-dioxane, a cyclic model compound for poly(propylene oxide),[47] and (set C) those obtained from density functional MO calculations at the B3LYP/6-311++G(3df, 3pd) level for EGDB itself. For sets A and B, $^3J_T = {}^3J'_T$ and $^3J_G = {}^3J'_G = {}^3J''_G$ were assumed. For the individual ^3J_T and ^3J_G values, see the footnote of Table 3. The p_t and p_g values derived from eqs 3 and 4 were divided by their sum to satisfy eq 2. The trans fractions thus obtained are listed in Table 3.

In the analysis for $^3J_{CH}$ with eqs 1 and 2, the three coefficients, ^3J_T, ^3J_G, and $^3J'_G$, were derived from (set a) the Karplus equation established for the C−O−C−H bond sequence of carbohydrates: $^3J_{COCH} = 5.7\cos^2\phi + 0.6\cos\phi + 0.5$ (ϕ: dihedral angle between ^{13}C and ^1H).[48] Then, the ϕ values were set equal to those optimized at the B3LYP/6-311+G(2d, p) level. In addition, the three ^3J coefficients obtained from the MO calculations for EGDB were used (see the footnote of Table 3).

For the CH_2-CH_2 bond of EGDB, the p_t values, depending on the ^3J coefficients used, are somewhat smaller than those ($p_t \sim 0.05$ (in water) to 0.2 (in cyclohexane)) of PEO and its model compounds.[4−7,46] The trans fraction of EGDB increases with temperature. In the all-trans conformation of EGDB, two dipole moments of the ester groups offset each other (see Figures 1 and 4), and then EGDB would be symmetric in electric charge. As shown in Table 3, therefore, nonpolar solvents tend to increase the p_t value of the CH_2-CH_2 bond.

On the other hand, the trans preference ($p_t \sim 0.4-0.5$) of the $O-CH_2$ bond is not so strong as found for PEO ($p_t \geq 0.65$). Schneider et at.[49] measured ^1H and ^{13}C NMR and Raman spectra of EGDB. The ^1H NMR methylene satellite band, observed at 200 MHz from the benzene solution, was analyzed according to a procedure employed for PEO[50] to yield $p_t = 0.05 - 0.09$ (at 25 °C) for the CH_2-CH_2 bond of the spacer. The p_t values agree with the results here. The Raman spectra of molten and glassy EGDB show intense bands (800 − 815 and 1400 − 1500 cm^{-1}) due to gg conformations in the CH_2-CH_2/CH_2-O bond pair. The spacer of EGDB somewhat differs from the $O-CH_2-CH_2-O$ bond sequence of PEO in conformational preference.

MO Calculations and Conformational Energies. Inasmuch as the phenyl ring and ester group of EGDB are coplanar, only bonds 5, 6, and 7 (see Figure 1) have the freedom of internal rotation. Under the RIS approximation, three conformations, t, g^+, and g^-, are defined for these bonds. The spacer has 27 conformations; however, the molecular symmetry reduces the number of independent conformers to 10. Conformer free energies (ΔG_k's) of the 10 conformers of EGDB and cis forms of DMT and DMN are shown in Table 4. Only for the $g^+g^-g^+$ conformer of EGDB, no potential minimum was found. Here, for example, the notation tg^+g^- represents that bonds 5, 6, and 7 adopt the t, g^+, and g^- conformations, respectively.

Table 3. Trans Fractions (p_t's) in the $O-CH_2-CH_2-O$ Bond Sequence of EGDB

		p_t				
		CH_2-CH_2			$O-CH_2$	
medium	temp (°C)	set A[a]	set B[b]	set C[c]	set a[d]	set b[e]
		NMR Experiment				
cyclohexane	15	0.11	0.08	0.18	0.43	0.42
	25	0.12	0.09	0.19	0.43	0.42
	35	0.13	0.09	0.20	0.42	0.41
	45	0.13	0.10	0.20	0.42	0.41
	55	0.13	0.10	0.21	0.41	0.40
benzene	15	0.08	0.03	0.15	0.48	0.45
	25	0.08	0.04	0.15	0.46	0.44
	35	0.09	0.05	0.16	0.45	0.43
	45	0.09	0.05	0.16	0.44	0.42
	55	0.10	0.06	0.17	0.44	0.42
methanol	15	0.05	0.02	0.12	0.42	0.41
	25	0.06	0.03	0.13	0.41	0.40
	35	0.07	0.04	0.14	0.41	0.40
	45	0.09	0.06	0.16	0.41	0.40
	55	0.09	0.06	0.16	0.40	0.39
dimethyl sulfoxide	15	0.04	0.01	0.11	0.49	0.46
	25	0.05	0.02	0.12	0.48	0.45
	35	0.06	0.02	0.13	0.48	0.45
	45	0.06	0.03	0.13	0.46	0.44
	55	0.07	0.04	0.14	0.44	0.42
		MO Calculation[e]				
gas phase	15	0.06			0.46	
	25	0.06			0.45	
	35	0.06			0.45	
	45	0.07			0.45	
	55	0.07			0.45	
benzene	15	0.05			0.49	
	25	0.05			0.49	
	35	0.06			0.49	
	45	0.06			0.48	
	55	0.06			0.48	

[a] Coupling constants optimized for poly(ethylene oxide): $^3J_T = 11.4$ and $^3J_G = 2.3$ Hz (ref 46). [b] Coupling constants from *cis*-2,6-dimethyl-1,4-dioxane, a model compound of poly(propylene oxide): in cyclohexane, $^3J_T = 9.80$ and $^3J_G = 2.54$ Hz; in benzene, $^3J_T = 9.87$ and $^3J_G = 2.54$ Hz; in methanol and dimethyl sulfoxide, $^3J_T = 10.25$ and $^3J_G = 2.52$ Hz (ref 47). [c] Coupling constants from MO calculations for EGDB at the B3LYP/6-311++G(3df, 3pd) level (this study): $^3J_T = 11.50$, $^3J_G = 4.90$, $^3J'_T = 10.96$, $^3J'_G = 1.48$, and $^3J''_G = 2.35$ Hz. [d] Coupling constants from the Karplus equation (ref 48): $^3J_G = 1.7$ Hz ($\phi = 120.5°$), $^3J'_T = 5.4$ Hz ($\phi = 28.8°$), and $^3J'_G = 4.0$ Hz ($\phi = 147.3°$). [e] Coupling constants from MO calculations for EGDB at the B3LYP/6-311++G(3df, 3pd) level (this study): $^3J_G = 1.17$, $^3J'_T = 6.31$, and $^3J'_G = 3.59$ Hz.

The p_t values of EGDB (Table 3), calculated from ΔG_k's for the gas phase and benzene solution, closely agree with the NMR experiments. If ΔG_k values of the ttg^+ and tg^+t conformers are considered to be first-order interaction energies (E_ρ and E_σ), that is, gauche energies of the $O-CH_2$ and CH_2-CH_2 bonds, respectively, then the higher-order interaction energy, E_{α_k}, of conformer k may be calculated from

$$E_{\alpha_k} = \Delta G_k - n_{\rho_k}E_\rho - n_{\sigma_k}E_\sigma \quad (5)$$

where n_{ρ_k} and n_{σ_k} are numbers of gauche conformations in the $O-CH_2$ and CH_2-CH_2 bonds of conformer k, respectively.

Therefore, the E_{α_k} parameter includes all higher-order interactions between atoms (atomic groups) separated by more than 3 bonds. The conformer free energies were divided into two first- (E_ρ and E_σ) and six higher-order (E_{α_k}, $k = 4-9$) interaction energies, of which values are given in Table 5.

As mentioned in the Introduction, by analogy with PEO, only three conformational energies, E_ρ, E_σ, and E_ω, have often been defined for the spacer of PET. If this definition may be applied to EGDB here, the following relations must be fulfilled: $E_{\alpha_4} \simeq E_{\alpha_6} \simeq E_{\alpha_7} \simeq E_{\alpha_8} \simeq$ null and $E_{\alpha_5} \simeq E_{\alpha_9}$ ($= E_\omega$); however, the data in Table 5 do not satisfy these conditions. Figure 4 illustrates the α_k interactions. In the figure, the dotted lines stand for nonbonded O···H contacts shorter than the sum (2.7 Å) of van der Waals radii of oxygen and hydrogen atoms.[51] Between two phenyl groups, four electronegative oxygen atoms are closely packed; therefore, electronic structures of all the conformers are complicated. For example, in the tg^+g^- conformation (Figure 4b), its left-hand phenyl and ester groups and a methylene C−H bond are coplanar, and the C═O···H−C spacing is as short as 2.24 Å; some attractive interaction is suggested to exist between the ester and methylene groups. The natural bond orbital (NBO) analysis[52,53] at the HF/6-311+G(2d, p) level evaluated partial charges of the oxygen and hydrogen atoms to be −0.71 and +0.20, respectively, and estimated the stabilization (attraction) energy due to the lone pair to C−H antibond ($n_O \rightarrow \sigma^*_{C-H}$) delocalization to be 0.55 kcal mol^{-1}. Some repulsion(s) may occur simultaneously and cancel out the attraction; the sum, $E_{\alpha 5}$, is negligible (−0.03 kcal mol^{-1} for the gas phase at 25 °C). The short O···H contact of 2.25 Å is also found in the $g^+g^+g^-$ conformation (Figure 4f). In the g^+tg^+ and g^+tg^- states, two dipole moments are, respectively, approximately parallel (unstable) and antiparallel (stable); the corresponding E_{α_k} values are 0.09 and −0.59 kcal mol^{-1}, respectively. As elucidated above, it is impossible to express conformational characteristics of EGDB and PET by only a few pairwise interactions between atomic groups. To apply the MO energies as they are to the RIS calculations,[54,55] this study has adopted the two first-order (E_ρ and E_σ) and six higher-order (E_{α_k}, $k = 4-9$) interaction energies and the following statistical weight matrices U_j's (j: bond number) for the spacer:

$$U_5 = \begin{bmatrix} 1 & \rho & \rho \\ 0 & 0 & 0 \\ 0 & 0 & 0 \end{bmatrix} \tag{6}$$

$$U_6 = \begin{bmatrix} 1 & \sigma & \sigma & 0 & 0 & 0 & 0 & 0 & 0 \\ 0 & 0 & 0 & 1 & \sigma & \sigma & 0 & 0 & 0 \\ 0 & 0 & 0 & 0 & 0 & 0 & 1 & \sigma & \sigma \end{bmatrix} \tag{7}$$

$$U_7 = \begin{bmatrix} 1 & \rho & \rho & 0 & 0 & 0 & 0 & 0 & 0 \\ 0 & 0 & 0 & 1 & \rho\alpha_4 & \rho\alpha_5 & 0 & 0 & 0 \\ 0 & 0 & 0 & 0 & 0 & 0 & 1 & \rho\alpha_5 & \rho\alpha_4 \\ 1 & \rho\alpha_6 & \rho\alpha_7 & 0 & 0 & 0 & 0 & 0 & 0 \\ 0 & 0 & 0 & \alpha_4 & \rho\alpha_8 & \rho\alpha_9 & 0 & 0 & 0 \\ 0 & 0 & 0 & 0 & 0 & 0 & \alpha_5 & 0 & \rho\alpha_9 \\ 1 & \rho\alpha_7 & \rho\alpha_6 & 0 & 0 & 0 & 0 & 0 & 0 \\ 0 & 0 & 0 & \alpha_5 & \rho\alpha_9 & 0 & 0 & 0 & 0 \\ 0 & 0 & 0 & 0 & 0 & 0 & \alpha_4 & \rho\alpha_9 & \rho\alpha_8 \end{bmatrix} \tag{8}$$

The statistical weights are calculated from the corresponding conformational energies according to, for example, $\alpha_k = \exp(-E_{\alpha_k}/RT)$, where R is the gas constant, and T is the absolute temperature.

Molar Kerr Constant. As outlined in the Introduction, the dipole moment and molar Kerr constant are also configuration-dependent parameters. Mendicuti et al.[34] measured the dipole moment of EGDB dissolved in benzene at 25 °C and the molar Kerr constant of the cyclohexane solution at 25 °C. To revalidate the MO calculations, it was attempted to reproduce the experimental dipole moment and molar Kerr constant of EGDB from the free energies, dipole moments, and polarizabilities that the MO calculations yielded.

The molar Kerr constant ${}_mK$ is expressed as[17]

$${}_mK = \frac{2\pi N_A}{15 k_B T}\left[\frac{\mu^T \hat{\alpha} \mu}{k_B T} + \mathrm{tr}(\hat{\alpha}\hat{\alpha})\right] \tag{9}$$

where N_A is Avogadro's number, k_B is Boltzmann's constant, and μ^T is the transpose of dipole moment μ, that is, $\mu^T = (\mu_x, \mu_y, \mu_z)$. The anisotropic part $\hat{\alpha}$ of the polarizability tensor α is given by

$$\hat{\alpha} = \alpha - \frac{1}{3}\mathrm{tr}(\alpha) I_3 \tag{10}$$

where

$$\alpha = \mathrm{diag}(\alpha_x, \alpha_y, \alpha_z) \tag{11}$$

and I_3 is the identity matrix of size 3. The Gaussian03 program[39] gives both dipole moment vector (μ_{MO}) and polarizability tensor (α_{MO}) with respect to the so-called standard orientation. The diagonalization of α_{MO} yields the above α tensor (its eigenvalues are α_x, α_y, and α_z), and the coordinate transformation to the principal-axis system defined by the resultant eigenvectors changes the μ_{MO} vector to the above μ. In this manner, we can derive both α tensor and μ vector to calculate the molar Kerr constant for each conformer. The observed molar Kerr constant $\langle {}_mK \rangle$ is related to the conformer free energies according to

$$\langle {}_mK \rangle = \sum_k {}_mK_k M_k \exp\left(-\frac{\Delta G_k}{RT}\right) / \sum_k M_k \exp\left(-\frac{\Delta G_k}{RT}\right) \tag{12}$$

where ${}_mK_k$ and M_k are the molar Kerr constant and multiplicity of conformer k, respectively. The average dipole moment is similarly derived from

$$\langle \mu \rangle = \sum_k \mu_k M_k \exp\left(-\frac{\Delta G_k}{RT}\right) / \sum_k M_k \exp\left(-\frac{\Delta G_k}{RT}\right) \tag{13}$$

where μ_k is the dipole moment of conformer k.

The μ_{MO} vectors and α_{MO} tensors were obtained from the MO calculations at the B3LYP/6-311+G(2d, p) level. Table 6 shows elements of the diagonalized polarizability tensors and the corresponding dipole moment vectors of the individual conformers. Substitution of the α tensors and μ vectors in Table 6 and the ΔG_k energies (benzene, 25 °C) in Table 4 into eqs 12 and 13 yielded $\langle {}_mK \rangle = 32.3 \times 10^{-25}$ m^5 V^{-2} mol^{-1} and $\langle \mu \rangle = 2.93$ D. These results slightly exceed the experimental values, $\langle {}_mK \rangle = 29.1 \pm 1.6 \times 10^{-25}$ m^5 V^{-2} mol^{-1} and $\langle \mu^2 \rangle^{1/2} = 2.75$ D,[34] but are fully satisfactory nevertheless, because the split-valence basis sets used here tend to somewhat overestimate dipole moments of compounds with polar groups. For molecules with ${}^+C{=}O^-$ polarities, for example, carbon monoxide, comparatively large discrepancies in μ and α between MO calculations and experiments have been found.[56] It is known that Dunning's cc-pVXZ[57] and Sadlej's POL[58] basis sets give dipole moments and polarizabilities more consistent with experiment. These basis sets were also used here for the μ_{MO} and α_{MO} calculations of EGDB; however, the expensive computations were always discontinued by the SCF failure, even though conditions for the density functional theory and SCF calculations were modified.

As shown above, the MO calculations satisfactorily reproduced both NMR and electric birefringence experiments. Therefore, conformational characteristics and configurational

Table 4. Free Energies (ΔG_k's) of Conformers of EGDB, DMT, and DMN, Evaluated by ab Initio MO Calculations

						ΔG_k,[a] kcal mol^{-1}		
						gas	benzene	
k	conformation[b]			multiplicity	statistical weight[c]	25 °C	25 °C	250 °C
					EGDB			
1	t	t	t	1	1	0.00	0.00	0.00
2	t	t	g^+	4	ρ	0.50	0.55	0.80
3	t	g^+	t	2	σ	−1.12	−1.24	−0.98
4	t	g^+	g^+	4	$\rho\sigma\alpha_4$	−0.96	−0.94	−0.82
5	t	g^+	g^-	4	$\rho\sigma\alpha_5$	−0.65	−0.69	−0.58
6	g^+	t	g^+	2	$\rho^2\alpha_6$	1.09	1.16	1.28
7	g^+	t	g^-	2	$\rho^2\alpha_7$	0.41	0.61	1.08
8	g^+	g^+	g^+	2	$\rho^2\sigma\alpha_8$	−0.84	−0.73	−0.19
9	g^+	g^+	g^-	4	$\rho^2\sigma\alpha_9$	−0.61	−0.59	−0.59
10	g^+	g^-	g^+	2	0	(absent)[d]		
					DMT			
cis					γ	0.16	0.15	0.16
					DMN			
cis					γ	0.28	0.28	0.19

[a] At the MP2/6-311+G(2d, p)//B3LYP/6-311+G(2d, p) level. Relative to the all-trans conformation. [b] In the O−CH_2−CH_2−O bond sequence of the spacer for EGDB. In the C(=O)−C−C−C(=O) bond sequence for DMT and DMN. [c] For the definitions, see Figures 1, 2, and 4. [d] The local minimum of the potential was not found by geometrical optimization at the B3LYP/6-311+G(2d, p) level.

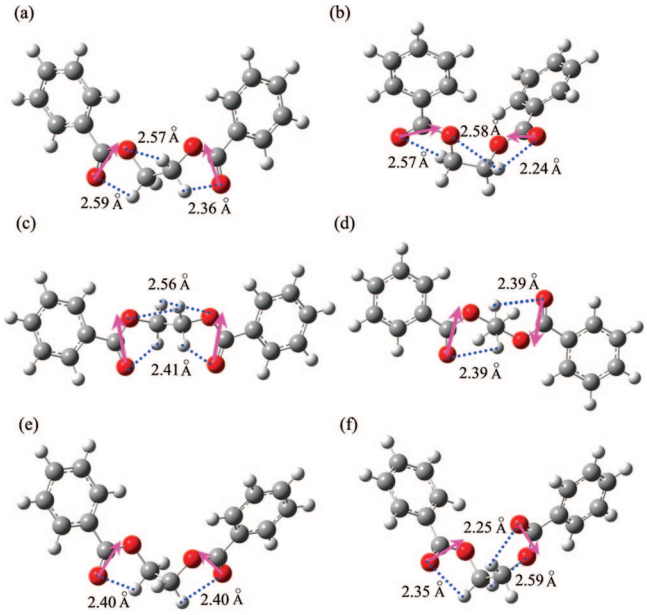

Figure 4. Higher-order intramolecular interactions formed in EGDB, PET, and PEN: (a) the α_4 interaction (in the tg^+g^+ conformation); (b) α_5 (tg^+g^-); (c) α_6 (g^+tg^+); (d) α_7 (g^+tg^-); (e) α_8 ($g^+g^+g^+$); (f) α_9 ($g^+g^+g^-$). The dotted lines stand for nonbonded O···H contacts shorter than the sum (2.7 Å) of van der Waals radii of oxygen and hydrogen atoms, and the numerical values are the O···H distances. The arrows express dipole moments of the ester groups.

properties of unperturbed PET and PEN may be investigated and discussed on the basis of the interaction energies established as above.

Characteristic Ratios of PET and PEN, Calculated by Refined RIS Scheme. When statistical weight matrices, U_j's, are formulated in the form of 9 × 9 for the RIS calculation, intramolecular interactions are expressed as a function of conformations of the current and two preceding bonds in the U_j matrices. The refined RIS scheme treats the bond length, bond angle, and dihedral angle as a function of conformations of the current, preceding, and subsequent bonds. As a consequence, the refined RIS scheme coupled with ab initio MO calculations has attained accurate a priori predictions of configurational properties of polymers.[42,43]

Table 5. Conformational Energies of EGDB, DMT, DMN, PET, and PEN, Evaluated by ab Initio MO Calculations

	conformational energy (kcal mol^{-1})		
	gas	benzene	
interaction[a]	25 °C	25 °C	250 °C
first-order			
ρ	0.50	0.55	0.80
σ	−1.12	−1.24	−0.98
higher-order			
α_4	−0.34	−0.25	−0.64
α_5	−0.03	0.00	−0.40
α_6	0.09	0.06	−0.32
α_7	−0.59	−0.49	−0.52
α_8	−0.72	−0.59	−0.81
α_9	−0.49	−0.45	−1.21
γ (DMT and PET)	0.16	0.15	0.16
γ (DMN and PEN)	0.28	0.28	0.19

[a] For the definitions, see Figures 1, 2, and 4.

Table 6. Dipole Moments (μ's) and Polarizabilities (α's) of Conformers of EGDB, Evaluated by ab Initio MO Calculations and Diagonalized with Respect to the Principal Axes (x, y, and z)[a]

				μ, D				α, Å^3		
k	conformation			x	y	z	total[b]	x	y	z
1	t	t	t	0.000	0.000	0.000	0.000	43.99	30.27	16.79
2	t	t	g^+	−0.198	−1.301	−2.029	2.418	44.21	23.80	23.14
3	t	g^+	t	0.000	2.644	0.000	2.644	36.16	30.88	22.66
4	t	g^+	g^+	−1.649	3.225	1.212	3.820	34.66	32.74	21.91
5	t	g^+	g^-	1.495	0.153	1.062	1.840	33.38	29.85	25.68
6	g^+	t	g^+	0.000	3.448	0.000	3.448	44.67	29.14	17.49
7	g^+	t	g^-	0.002	0.001	0.002	0.003	44.70	29.48	17.16
8	g^+	g^+	g^+	0.000	3.203	0.000	3.203	36.74	32.23	20.45
9	g^+	g^+	g^-	−2.775	−0.288	−1.915	3.384	35.04	31.05	22.67
10	g^+	g^-	g^+				(absent)[c]			

[a] At the B3LYP/6-311+G(2d, p) level. [b] $\mu_{total}^2 = \mu_x^2 + \mu_y^2 + \mu_z^2$. [c] The local minimum of the potential was not found by the geometrical optimization.

According to Williams and Flory,[3] a virtual bond has been defined for the aromatic ring. The line segment connecting two carbonyl carbons attached to the same aromatic ring is treated as if to be a long C−C bond (bonds 3 and b in Figure 1). The virtual bond of PET coincides with the para axis, whereas, for PEN, the length and angle of the virtual bond depend on the trans−cis orientation. In the refined RIS scheme, the geometrical parameters are set separately for the two arrangements and averaged by statistical weights. Inasmuch as PEN is different

Table 7. Characteristic Ratios and Bond Conformations of PET and PEN and Thermodynamic Quantities of Fusion of PET, PEN, and PEO, Evaluated from Refined RIS Calculations

		PET			PEN		PEO
		25 °C	250 °C	553 K[a]	25 °C	610 K[a]	342 K[a]
$\langle r^2\rangle_0/nl^2$ for $x\rightarrow\infty$		2.63	2.84	2.87	2.43	2.55	
trans fraction (p_t)	bond a	1.00	1.00	1.00	1.00	1.00	
	bond b	0.56	0.54	0.54	0.62	0.54	
	bond c	1.00	1.00	1.00	1.00	1.00	
	bond d	0.49	0.43	0.43	0.49	0.43	
	bond e	0.05	0.12	0.13	0.05	0.14	
	bond f	0.49	0.43	0.43	0.49	0.43	
S_{conf}, cal K^{-1} mol^{-1}		7.12	7.48	7.51	7.08	7.55	5.02
U_{conf}, kcal mol^{-1}		−0.76	−0.44	−0.43	−0.71	−0.39	0.64
ΔS_u,[b] cal K^{-1} mol^{-1}				11.6		9.80	6.04
ΔH_u,[b] kcal mol^{-1}				6.41		5.98	2.07

[a] Equilibrium melting points (refs 59–61). [b] Experimental values of entropy (ΔS_u) and enthalpy (ΔH_u) of fusion (ref 60).

Table 8. Average Geometrical Parameters of PET and PEN at 25 °C, Obtained from MO and Refined RIS Calculations,[a] and X-ray Crystallographic Data on EGDB

	MO and refined RIS		X-ray
	PET	PEN	EGDB[b]
	Bond Length, Å		
$l_{O-C(=O)}$	1.357	1.358	1.339
$l_{C(=O)-C(=O)}$[c]	5.778	7.984	5.72
l_{O-CH_2}	1.439	1.439	1.442
$l_{CH_2-CH_2}$	1.515	1.516	1.499
	Bond Angle, deg		
$\angle OC(=O)C(=O)$[c]	114.2	119.6	113.0
$\angle C(=O)OCH_2$	116.0	116.1	115.7
$\angle OCH_2CH_2$	109.8	109.7	105.0
	Dihedral Angle, deg		
$\phi_{cis}(C(=O)-C(=O))$[c]	180.0	180.0	
$\phi_{g\pm}(O-CH_2)$	±89.6	±90.1	
$\phi_{g\pm}(CH_2-CH_2)$	±114.6	±114.9	

[a] Using the conformational energies for benzene solutions at 25 °C (Table 5) and geometrical parameters of model compounds (Tables S1 and S2, Supporting Information). [b] The EGDB molecule adopts a quasi all-trans conformation (ref 62). [c] Virtual bonds for the aromatic rings.

from PET only in aromatic ring, the conformational energies, E_ρ, E_σ, and E_{α_k}'s, may be common to PET and PEN. In actuality, this assumption was confirmed to be valid by comparison of SCF energies of ethyleneglycol bis(dimethyl terephthalate) and ethyleneglycol bis(dimethyl 2,6-naphthalate). Only the E_γ value was set separately. Statistical weight matrices of bonds 2 − 7 and a−f, formulated in the 9 × 9 form, are given in Appendix S1 (Supporting Information). The geometrical parameters shown in Tables S1 and S2, and the conformational energies in Table 5 were used in the refined RIS calculations. Configuration-dependent parameters of PET and PEN at 25 °C, 250 °C, 553 K (equilibrium melting point, T_m, of PET),[59,60] and 610 K (T_m of PEN)[59,61] were derived from the conformational energies for benzene environments at 25, 250, 250, and 250 °C, respectively. The results are summarized in Table 7, and their averaged geometrical parameters are compared with those of crystallized EGDB[62] in Table 8.

The characteristic ratios of the infinite chains (degree of polymerization, $x \rightarrow \infty$) of PET at 25 and 250 °C, determined from extrapolation to $x^{-1} \rightarrow 0$ of $\langle r^2\rangle_0/nl^2$ vs x^{-1} plot, are 2.63 and 2.84, respectively. The $\langle r^2\rangle_0/nl^2$ values (Table 1) estimated from the good solutions are generally larger than those calculated here. As mentioned above, the NMR spectra of EGDB dissolved in TFA suggest the existence of some solute−solvent interaction. In viscosity measurements of PET, acids such as TFA, phenol, *o*-chlorophenol, and dichloroacetic acid have always been used. These acids may be selectively absorbed to PET, interfere with the intramolecular attractions (Figure 4), and disturb its intrinsic conformations. This is probably the reason why the extrapolations of viscometric data did not yield results consistent with this study. We have occasionally discussed such strong solvent effects.[63−65] The solubility of polymers forming attractive interactions is often due to intramolecular-to-intermolecular transfers of the attractions, and these transfers mostly enlarge the polymer dimension.

The $\langle r^2\rangle_0/nl^2$ value (2.84) of PET at 250 °C falls within the range of those determined by SANS for molten PET at 250 °C: 2.7 (Zimm plot); 3.1 (Kratky plot).[29] Imai et al.[66] determined the $\langle r^2\rangle_0/nl^2$ value of melt-quench PET to be 3.1; the sample was melt pressed at 285 °C for 2 min, quenched in ice water, annealed at 88 °C, quenched again in ice water, and underwent an SANS measurement. The $\langle r^2\rangle_0/nl^2$ value is slightly larger than the present data (2.87) at 280 °C, because the sample was annealed after the first quenching. It is well established that configurational properties of unperturbed polymers are determined only from short-range intramolecular interactions and that molten polymers are unperturbed. The molten PET chain may be expressed by the conformational energies for the benzene environment, because the dielectric constant (3.2) of PET at room temperature is close to that (2.3) of benzene. Accordingly, this agreement between theory and experiment should be accepted as a solid fact. The $\langle r^2\rangle_0/nl^2$ values of PEN at 25 °C and 610 K were calculated to be 2.43 and 2.55, respectively.

Thermodynamic Quantities of Fusion. The configurational entropy (S_{conf}) and intramolecular energy (U_{conf}) per monomer mole are given by[67]

$$S_{conf} = \frac{R}{x}\left[\ln Z + T\frac{d(\ln Z)}{dT}\right] \tag{14}$$

and

$$U_{conf} = \frac{RT^2}{x}\frac{d(\ln Z)}{dT} \tag{15}$$

The partition function of the whole chain, Z, is calculated from

$$Z = J^*\left(\prod_{j=2}^{n-1} U_j\right)J \tag{16}$$

where J^* is the row matrix of which first element is unity and the others are null, and J is the column matrix whose elements are unity.[54,55] The S_{conf} and U_{conf} values, respectively, correspond to the configurational entropy and intramolecular energy of the Θ state relative to the crystalline state at a temperature T, and the crystal is assumed to be perfect; therefore, $S_{cryst} = 0$ and $U_{cryst} = 0$.

At the equilibrium melting point, T_m, the enthalpy ΔH_u and entropy ΔS_u of fusion are related by

$$\Delta H_u = T_m \Delta S_u \quad (17)$$

Mandelkern has expressed the entropy of fusion in a phenomenological way:[68]

$$\Delta S_u = (\Delta S_u)_V + \Delta S_V \quad (18)$$

where the isovolumetric entropy of fusion, $(\Delta S_u)_V$, may be equivalent to S_{conf}, and the entropy of volume change, ΔS_V, depends on the thermal expansion coefficient (α) and compressibility (β): $\Delta S_V = (\alpha/\beta)\Delta V_m$. Wunderlich has interpreted the entropy of fusion in terms of molecular mobility:[69]

$$\Delta S_u = S_{conf} + \Delta S_{ori} + \Delta S_{pos} \quad (19)$$

where ΔS_{ori} and ΔS_{pos} are entropy changes due to orientational and positional shifts, respectively. The difference between ΔS_u and S_{conf} may be considered to be the intermolecular entropy change.

In Table 7, the S_{conf} and U_{conf} values of PET and PEN, thus calculated, are shown. For the sake of comparison, the corresponding thermodynamic data on PEO are also given in Table 7. The $S_{conf}/\Delta S_u$ ratio of PET, a measure of the intramolecular effect on the overall structural change, is 0.65, being slightly smaller than those (0.8−0.9) of simple polyethers and polysulfides.[67] The U_{conf} value of PET is −0.43 kcal mol^{-1}. This means a peculiar fact that the molten PET chain itself is more stable by 0.43 kcal mol^{-1} than its crystalline state. Our previous studies[67] on polyethers, polysulfides, and polyselenoethers have always given only positive U_{conf} values.

It is known that PEN has two crystal modifications:[70,71] α form, in which the molecular chain adopts the all-trans conformation; β form, in which the spacer includes appreciable gauche conformations. The S_{conf} and U_{conf} values of the α form were calculated to be 7.55 cal K^{-1} mol^{-1} and −0.39 kcal mol^{-1}, respectively. Because the β form includes the structural defect, gauche bonds, the S_{conf} value is reduced to $(7.55 - S_\beta)$ cal K^{-1} mol^{-1}, where S_β is the residual configurational entropy in the β phase. The U_{conf} energy of the β form increases with increasing gauche CH_2-CH_2 bond.

In the previous paper,[67] we have stated that linear polymers tend to crystallize in the most stable conformation. However, PET and PEN are the exceptions, or otherwise the rule may possibly hold only for polymers without complicated chemical bonds in the skeleton. The conformational preferences of PET and PEN lead to the negative U_{conf}'s, whereas PEO with the same $O-CH_2-CH_2-O$ bond sequence, crystallizing into the stable tgt conformation, has a positive U_{conf} of 0.64 kcal mol^{-1}. Without the aid of effective intermolecular stabilizations, the polyesters can not shift the spacer conformation from the gauche-rich to trans-rich state and crystallize in the all-trans structure.[70,72] This is a reason why PET (PEN) forms a paracrystalline state (the β form) including gauche bonds[70,71,73,74] and why crystallization of these polyesters is so slow as to be investigated by a variety of analytical methods on human time scales.[75]

Conclusions

Conformational characteristics and configurational properties of PET and PEN have been elucidated by ab initio MO calculations and ^{1}H and ^{13}C NMR experiments for EGDB and the refined RIS calculations for the polyesters. The MO calculations satisfactorily reproduced experimental observations of NMR, dipole moment, and molar Kerr constant of EGDB. Intermolecular interactions formed in EGDB, PET, and PEN are too complicated to be simply interpreted on the analogy of those of PEO. The refined RIS calculations for PET with the MO energies of EGDB yielded characteristic ratios that exactly agree with those determined from SANS experiments for the melt. On the basis of thermodynamic quantities obtained from the RIS calculations, melting and crystallization of PET and PEN have been discussed. The first-principles calculations for the model compounds, via statistical mechanics and thermodynamics, have led us to accurate understanding of conformational characteristics, configurational properties, and thermodynamic properties of the polyesters. At length, we have acquired the most fundamental physicochemical information about the mass-produced polyesters.

Supporting Information Available: Statistical weight matrices of EGDB, PET, and PEN (Appendix S1) and geometrical parameters used in the refined RIS calculations for PET and PEN (Tables S1 and S2, respectively). This material is available free of charge via the Internet at http://pubs.acs.org.

References and Notes

(1) Iroh, J. O. Poly(ethylene terephthalate). In *Polymer Data Handbook*; Mark, J. E., Ed.; Oxford University Press: New York, 1999; p 558.
(2) Iroh, J. O. Poly(ethylene-2,6-naphthalate). In *Polymer Data Handbook*; Mark, J. E., Ed.; Oxford University Press: New York, 1999; p 540.
(3) Williams, A. D.; Flory, P. J. *J. Polym. Sci., A-2* **1967**, *5*, 417.
(4) Mark, J. E.; Flory, P. J. *J. Am. Chem. Soc.* **1965**, *87*, 1415.
(5) Abe, A.; Mark, J. E. *J. Am. Chem. Soc.* **1976**, *98*, 6468.
(6) Abe, A.; Tasaki, K.; Mark, J. E. *Polym. J.* **1985**, *17*, 883.
(7) (a) Sasanuma, Y.; Ohta, H.; Touma, I.; Matoba, H.; Hayashi, Y.; Kaito, A. *Macromolecules* **2002**, *35*, 3748. (b) Sasanuma, Y.; Sugita, K. *Polym. J.* **2006**, *38*, 983.
(8) The ρ, σ, and ω interactions, whose designations are consistent with those for PEO, were, respectively, termed σ_κ, σ_η, and $\omega_{\eta\kappa}$ in the original paper.[3]
(9) In the present paper, the experimental $\langle r^2\rangle_0/nl^2$ values are recalculated with use of bond lengths determined here (Table 8). It should be noted that the $\langle r^2\rangle_0/nl^2$ values here can not be simply compared with those of other polymers, because a virtual-bond length is included in $\langle r^2\rangle_0/nl^2$'s of PET and PEN. Williams and Flory[3] modified the original $\langle r^2\rangle_0/nl^2$ value reported by Lanka and Krigbaum;[10] a different viscosity constant (Φ) was employed.
(10) (a) Krigbaum, W. R. *J. Polym. Sci.* **1958**, *28*, 213. (b) Krigbaum, W. R. *J. Polym. Sci.* **1955**, *18*, 315.
(11) Kurata, M.; Stockmayer, W. H. *Fortschr. Hochpolym.-Forsch.* **1963**, *3*, 196.
(12) Stockmayer, W. H.; Fixman, M. *J. Polym. Sci., Part C* **1963**, *1*, 137.
(13) Wallach, M. L. *Makromol. Chem.* **1967**, *103*, 19.
(14) Aharoni, S. M. *Makromol. Chem.* **1978**, *179*, 1867.
(15) Meyerhoff, G.; Shimotsuma, S. *Makromol. Chem.* **1970**, *135*, 195.
(16) Tuzar, Z.; Vosicky, V.; Bohdanecky, M. *Makromol. Chem.* **1979**, *180*, 1399.
(17) Riande, E.; Saiz, E. *Dipole Moments and Birefringence of Polymers*; Prentice Hall: Englewood Cliffs, NJ, 1992, and references therein.
(18) Nagai, K.; Ishikawa, T. *J. Chem. Phys.* **1965**, *43*, 4508.
(19) Flory, P. J.; Jernigan, R. L. *J. Chem. Phys.* **1968**, *48*, 3823.
(20) Suter, U. W.; Flory, P. J. *J. Chem. Soc., Faraday Trans. 2* **1977**, *73*, 1521.
(21) Saiz, E.; Suter, U. W.; Flory, P. J. *J. Chem. Soc., Faraday Trans. 2* **1977**, *73*, 1538.
(22) Tonelli, A. E. *Macromolecules* **1977**, *10*, 153.
(23) Kelly, K. M.; Patterson, G. D.; Tonelli, A. E. *Macromolecules* **1977**, *10*, 859.
(24) Saiz, E.; Hummel, J. P.; Flory, P. J.; Plavsic, M. *J. Phys. Chem.* **1981**, *85*, 3211.
(25) Irvine, P. A.; Erman, B.; Flory, P. J. *J. Phys. Chem.* **1983**, *87*, 2929.
(26) Flory, P. J. *Pure Appl. Chem.* **1984**, *56*, 305.
(27) Higgins, J. S.; Benoit, H. C. *Polymers and Neutron Scattering*; Oxford University Press: New York, 1994.
(28) Roe, R. J. *Methods of X-ray and Neutron Scattering in Polymer Science*; Oxford University Press: New York, 2000.
(29) Gilmer, J. W.; Wiswe, D.; Zachmann, H. G.; Kugler, J.; Fischer, E. W. *Polymer* **1986**, *27*, 1391.
(30) Wu, W.; Wiswe, D.; Zachmann, H. G.; Hahn, K. *Polymer* **1985**, *26*, 655.
(31) McAlea, K. P.; Schultz, J. M.; Gardner, K. H.; Wignall, G. D. *Macromolecules* **1985**, *18*, 447.
(32) Riande, E.; Guzman, J.; De La Campa, J. G.; De Abajo, J. *J. Polym. Sci., Part B: Polym. Phys.* **1987**, *25*, 2403.
(33) (a) Mendicuti, F.; Viswanadhan, N.; Mattice, W. L. *Polymer* **1988**, *29*, 875. (b) Bahar, I.; Mattice, W. L. *J. Chem. Phys.* **1989**, *90*, 6783.

(34) Mendicuti, F.; Rodrigo, M. M.; Tarazona, M. P.; Saiz, E. *Macromolecules* **1990**, *23*, 1139.
(35) Auriemma, F.; Corradini, P.; Guerra, G.; Vacatello, M. *Macromol. Theory Simul.* **1995**, *4*, 165.
(36) (a) Taylor, D. J. R.; Stepto, R. F. T.; Bleackley, M.; Ward, I. M. *Phys. Chem. Chem. Phys.* **1999**, *1*, 2065. (b) Cail, J. I.; Stepto, R. F. T.; Taylor, D. J. R.; Jones, R. A.; Ward, I. M. *Phys. Chem. Chem. Phys.* **2000**, *2*, 4361.
(37) (a) Tonelli, A. E. *J. Polym. Sci., Part B: Polym. Phys.* **2002**, *40*, 1254. (b) Tonelli, A. E. *Polymer* **2002**, *43*, 637.
(38) Kamio, K.; Moorthi, K.; Theodorou, D. N. *Macromolecules* **2007**, *40*, 710.
(39) Frisch, M. J.; Trucks, G. W.; Schlegel, H. B.; Scuseria, G. E.; Robb, M. A.; Cheeseman, J. R.; Montgomery, Jr., J. A.; Vreven, T.; Kudin, K. N.; Burant, J. C.; Millam, J. M.; Iyengar, S. S.; Tomasi, J.; Barone, V.; Mennucci, B.; Cossi, M.; Scalmani, G.; Rega, N.; Petersson, G. A.; Nakatsuji, H.; Hada, M.; Ehara, M.; Toyota, K.; Fukuda, R.; Hasegawa, J.; Ishida, M.; Nakajima, T.; Honda, Y.; Kitao, O.; Nakai, H.; Klene, M.; Li, X.; Knox, J. E.; Hratchian, H. P.; Cross, J. B.; Bakken, V.; Adamo, C.; Jaramillo, J.; Gomperts, R.; Stratmann, R. E.; Yazyev, O.; Austin, A. J.; Cammi, R.; Pomelli, C.; Ochterski, J. W.; Ayala, P. Y.; Morokuma, K.; Voth, G. A.; Salvador, P.; Dannenberg, J. J.; Zakrzewski, V. G.; Dapprich, S.; Daniels, A. D.; Strain, M. C.; Farkas, O.; Malick, D. K.; Rabuck, A. D.; Raghavachari, K.; Foresman, J. B.; Ortiz, J. V.; Cui, Q.; Baboul, A. G.; Clifford, S.; Cioslowski, J.; Stefanov, B. B.; Liu, G.; Liashenko, A.; Piskorz, P.; Komaromi, I.; Martin, R. L.; Fox, D. J.; Keith, T.; Al-Laham, M. A.; Peng, C. Y.; Nanayakkara, A.; Challacombe, M.; Gill, P. M. W.; Johnson, B.; Chen, W.; Wong, M. W.; Gonzalez, C.; Pople, J. A *Gaussian03*, revision D.01. Gaussian, Inc.: Wallingford, CT, 2004.
(40) Cances, E.; Mennucci, B.; Tomasi, J. *J. Chem. Phys.* **1997**, *107*, 3032.
(41) Mennucci, B.; Cances, E.; Tomasi, J. *J. Phys. Chem. B* **1997**, *101*, 10506.
(42) Sasanuma, Y.; Asai, S.; Kumagai, R. *Macromolecules* **2007**, *40*, 3488.
(43) Sasanuma, Y.; Kumagai, R. *Macromolecules* **2007**, *40*, 7393.
(44) Reimschuessel, H. K.; Debona, B. T.; Murthy, A. K. S. *J. Polym. Sci., Polym. Chem.* **1979**, *17*, 3217.
(45) Budzelaar, P. H. M. *gNMR*, version 5.0. IvorySoft & Adept Scientific plc: Letchworth, U.K., 2004.
(46) Tasaki, K.; Abe, A. *Polym. J.* **1985**, *17*, 641.
(47) Sasanuma, Y. *J. Phys. Chem.* **1994**, *98*, 13486.
(48) Tvaroska, I.; Hricovini, M.; Petrakova, E. *Carbohydr. Res.* **1989**, *189*, 359.
(49) Schneider, B.; Sedlacek, P.; Stokr, J.; Doskocilova, D. *Collect. Czech. Chem. Commun.* **1981**, *46*, 1913.
(50) Matsuzaki, K.; Ito, H. *J. Polym. Sci., Polym. Phys.* **1974**, *12*, 2507.
(51) Bondi, A. *J. Phys. Chem.* **1964**, *68*, 441.
(52) Reed, A. E.; Curtiss, L. A.; Weinhold, F. *Chem. Rev.* **1988**, *88*, 899.
(53) Glendening, E. D.; Reed, A. E.; Carpenter, J. E.; Weinhold, F. *NBO* version 3.1; Theoretical Chemistry Institute and Department of Chemistry, University of Wisconsin: Madison, WI.
(54) Flory, P. J. *Statistical Mechanics of Chain Molecules*; Wiley & Sons: New York, 1969.
(55) Mattice, W. L.; Suter, U. W. *Conformational Theory of Large Molecules: The Rotational Isomeric State Model in Macromolecular Systems*; Wiley & Sons: New York, 1994.
(56) Koch, W.; Holthausen, M. C. *A Chemist's Guide to Density Functional Theory*; Wiley-VCH: Weinheim, Germany, 2000; Chapter 10.
(57) (a) Dunning, T. H., Jr. *J. Chem. Phys.* **1989**, *90*, 1007. (b) Wilson, A. K.; van Mourik, T.; Dunning, T. H., Jr. *J. Mol. Struct. (THEOCHEM)* **1996**, *388*, 339, and references therein.
(58) (a) Sadlej, A. J. *Collect. Czech. Chem. Commun.* **1988**, *53*, 1995. (b) Sadlej, A. J. *Theor. Chim. Acta* **1991**, *79*, 123.
(59) Cheng, S. Z. D.; Wunderlich, B. *Thermochim. Acta* **1988**, *134*, 161.
(60) Wunderlich, B.; Gaur, U. *Pure Appl. Chem.* **1980**, *52*, 445.
(61) Cheng, S. Z. D.; Wunderlich, B. *Macromolecules* **1988**, *21*, 789.
(62) Perez, S.; Brisse, F. *Acta Crystallogr. B* **1976**, *32*, 470.
(63) Sasanuma, Y.; Hayashi, Y.; Matoba, H.; Touma, I.; Ohta, H.; Sawanobori, M.; Kaito, A. *Macromolecules* **2002**, *35*, 8216.
(64) Sasanuma, Y.; Hattori, S.; Imazu, S.; Ikeda, S.; Kaizuka, T.; Iijima, T.; Sawanobori, M.; Azam, M. A.; Law, R. V.; Steinke, J. H. G. *Macromolecules* **2004**, *37*, 9169.
(65) Sasanuma, Y.; Kumagai, R.; Nakata, K. *Macromolecules* **2006**, *39*, 6752.
(66) Imai, M.; Kaji, K.; Kanaya, T.; Sakai, Y. *Phys. Rev. B* **1995**, *52*, 12696.
(67) Sasanuma, Y.; Watanabe, A.; Tamura, K. *J. Phys. Chem. B* **2008**, *112*, 9613, and references therein.
(68) Mandelkern, L. *Crystallization of Polymers*; McGraw-Hill: New York, 1964; Chapter 5.
(69) Wunderlich, B. *Prog. Polym. Sci.* **2003**, *28*, 383.
(70) Buchner, S.; Wiswe, D.; Zachmann, H. G. *Polymer* **1989**, *30*, 480.
(71) Vasanthan, N.; Salem, D. R. *Macromolecules* **1999**, *32*, 6319.
(72) Daubeny, R. de P.; Bunn, C. W.; Brown, C. J. *Proc. R. Soc. London, A* **1954**, *226*, 531.
(73) (a) Bonart, R. *Kolloid Z. Z. Polym.* **1964**, *199*, 136. (b) Bonart, R. *Kolloid Z. Z. Polym.* **1966**, *213*, 1.
(74) Asano, T.; Seto, T. *Polym. J.* **1973**, *5*, 72.
(75) For example (a) Heffelfinger, C. J.; Schmidt, P. G. *J. Appl. Polym. Sci.* **1965**, *9*, 2661. (b) Cunningham, A.; Ward, I. M. *Polymer* **1974**, *15*, 749. (c) D'esposito, L.; Koenig, J. L. *J. Polym. Sci., Polym. Phys.* **1976**, *14*, 1731. (d) Lin, S. B.; Koenig, J. L. *J. Polym. Sci., Polym. Phys.* **1982**, *20*, 2277. (e) Yazdanian, M.; Ward, I. M.; Brody, H. *Polymer* **1985**, *26*, 1779. (f) Shen, D.; Long, F.; Wen, Z.; Qian, R. *Makromol. Chem.* **1991**, *192*, 301. (g) Murthy, N. S.; Correale, S. T.; Minor, H. *Macromolecules* **1991**, *24*, 1185. (h) Spiby, P.; O'Neill, M. A. O.; Duckett, R. A.; Ward, I. M. *Polymer* **1992**, *33*, 4479. (i) Guevremont, J.; Ajji, A.; Cole, K. C.; Dumoulin, M. M. *Polymer* **1995**, *36*, 3385. (j) Rodriguez-Cabello, J. C.; Merino, J. C.; Quintanilla, L.; Pastor, J. M. *J. Appl. Polym. Sci.* **1996**, *62*, 1953. (k) Ivanov, D. A.; Amalou, Z.; Magonov, S. N. *Macromolecules* **2001**, *34*, 8944. (l) Ran, S.; Wang, Z.; Burger, C.; Chu, B.; Hsiao, B. S. *Macromolecules* **2002**, *35*, 10102. (m) Haubruge, H. G.; Jonas, A. M.; Legras, R. *Macromolecules* **2004**, *37*, 126.

MA802804N